N. Jb. Miner. Abh. 189/1, 21–34
Published online November 2011

Article

Origin of analcime in the Neogene Arikli Tuff, Biga Peninsula, NW Turkey

Sevgi Ozen and M. Cemal Goncuoglu

With 8 figures and 3 tables

Abstract: The Arikli Tuff in the Behram Volcanics, NW Anatolia, is characterized by its dominance of authigenic analcime. It was studied by optical microscopy, XRD, SEM/EDX, and ICP for a better understanding of the analcime formation, which occurs as coarse-grained euhedral to subhedral crystals in pores and pumice fragments as well as in clusters or fine-grained single crystals embedded in the matrix. Besides analcime, K-feldspar, dolomite, and smectite are found as further authigenic minerals. Based on the dominance of these authigenic minerals, the tuffs are petrographically separated into phyllosilicate-bearing vitric tuff, dolomite-rich vitric tuff, and K-feldspar-dominated vitric tuff. No precursor of zeolites other than analcime was detected. Petrographical and SEM investigations indicate that euhedral to subhedral analcime crystals found as a coarse-grained filling cement in voids and pumice fragments are precipitated from pore water, whereas fine-grained disseminated crystals are formed by the dissolution-precipitation of glassy material. Hydrolysis of glassy material that is similar in composition to analcime provides the additional Na, Al, Si, and K elements which are necessary for the formation of analcime.

Key words: Alteration, analcime, Neogene tuff, NW Turkey, volcanic glass.

Introduction

Tuffs deposited in lacustrine conditions present a unique opportunity to study the zeolite-forming processes. Interaction of fluids with highly reactive glassy material is considered ideal for the formation of zeolites including analcime. As analcime forming mechanisms, generation from volcanic glass (Larsen et al. 1991, High & Picard 1965, Iijima &Utada 1966), from precursor alkali zeolites derived from volcanic glass (Hay 1966, Iijima & Hay 1968, Sheppard & Gude 1968, Surdam & Sheppard 1978), and from feldspars and clay minerals (Hay & Sheppard 2001) are proposed. Direct precipitation from saline, alkaline lake water (Hay 1966, Remy & Ferrel 1989, Renaut 1993, English 2001) was also suggested where tuffaceous material is absent and where zeolite is laterally widespread (Hay 1966).

Among a number of zeolites, analcime and clinoptilolite are the most common ones in Tertiary sediments of central and western Anatolia (Ataman & Gundogdu 1982 and references therein). Relatively important analcime-bearing tuff occurrences are at Bigadic (Emirler), Emet (Kopenez), Kirka (Karaoren), Urla, Bahcecik-Golpazari-Goynuk, Nallihan-Cayirhan-Beypazari-Mihaliccik, Kalecik-Hasayaz-Sabanozu-Candir, Polatli-Mülk-Oglakci-Ayas, Kesan, and Gordes regions (Ataman & Gundogdu 1982, Esenli & Ozpeker 1993, Gundogdu et al. 1996, Esenli et al. 2005), some of which extend over an area of approximately 2000 km^2 (Ataman & Gundogdu 1982). Although occurrence of analcime is common in Neogene volcaniclastic units in the Biga Peninsula, detailed mineralogical studies are not available.

This study aims to report the characteristics of analcime in the Arikli Tuff, and to discuss the diagenetic processes that lead to their formation. We investigated the mineralogy and geochemistry of representative Arikli Tuff samples to understand the relationship between coexisting phases. In addition, we examined changes in the original and authigenic minerals by electron microscopy with the aim of establishing the possible mechanism in analcime authigenesis.

Direct precipitation from saline, alkaline lake water (Hay 1966, Remy & Ferrel 1989, Renaut 1993, English 2001) or from a mixture of seawater and meteoric water

DOI: 10.1127/0077-7757/2011/0207
www.schweizerbart.de
0077-7757/2011 /0207 $ 3.50

with magmatic water enriched in Na and K (Abdioglu, this volume) was also suggested where tuffaceous material is absent and where zeolite is laterally widespread (Hay 1966).

Geological setting

The study area is located on the Biga Peninsula between Ayvacik and Kucukkuyu to the southeast of Troy in Canakkale, NW Turkey (Fig. 1) and covers an area of approximately 7 km^2.

The geology of the Biga Peninsula has been reported by a number of authors considering different geological aspects (Borsi et al. 1972, Bingol et al. 1973, Siyako et al. 1989, Okay et al. 1990, Ercan et al. 1995, Yilmaz et al. 2001 and Ciftci et al. 2004).

In brief, rock units exposed around Kucukkuyu and Ayvacik include the ophiolitic basement (Goncuoglu et al 1997), volcanics (Behram Volcanics), lacustrine sediments (Kucukkuyu Formation), and alluvium (Fig. 2). The basement is disconformably overlain by Lower-Middle Miocene calc-alkaline volcanic rocks (Behram Volcanics, Borsi et al. 1972, Ercan et al. 1995) and detrital sediments. The main rock-types of the Behram Volcanics are tuff, andesite, and andesitic agglomerate. They occur within a thick pile of sedimentary rocks that are collectively known as the Kucukkuyu Formation (Inci 1984, Siyako et al. 1989, Ciftci et al. 2004). The Kucukkuyu Formation is represented by well-bedded and yellowish brown, light grey, and greenish brown laminated lacustrine sediments. Dominant rock types are claystone, mudstone, and shale. The age of Kucukkuyu Formation is Early Miocene based on radiometric age data (Inci 1984) from the associated volcanic rocks.

The dacitic-rhyolitic tuffaceous rocks within the Behram Volcanics were named Arikli Tuff by Ciftci et al. (2004). The Arikli Tuff represents the main pyroclastic products of the volcanic activity and covers mainly the southern part of the study area. The massive and bedded tuffs are white, light green, yellow, and light yellow in color and range in thickness from laminae to a few meters. Although the tuff is fairly hard and compact in general, very fragile tuffs were also observed along the Neotectonic Edremit Fault Zone (Fig. 2). Siliceous nodules, 2–7 cm in diameter, occur sporadically in the Arikli Tuff. Analcime-rich samples are concentrated in the central part of the E-W trending Kucukkuyu lacustrine basin, where deeper lake sediments (Ciftci et al. 2004) such as laminated shales, marls, and siltstones with tuff interlayers dominate.

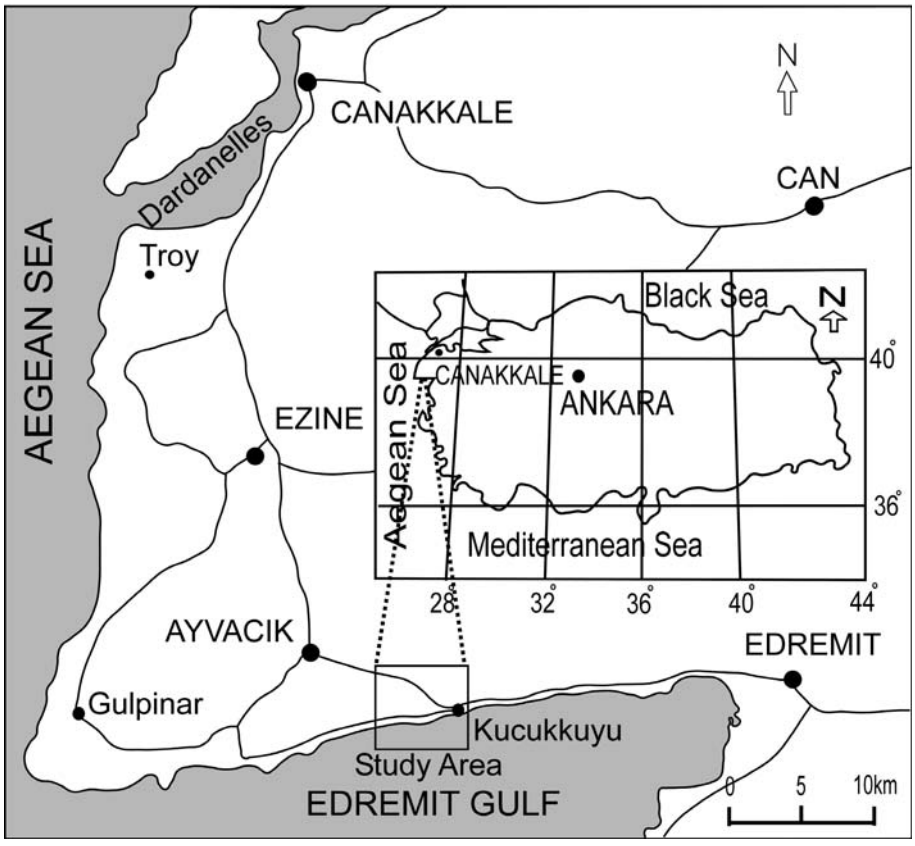

Fig. 1. Location map of the study area.

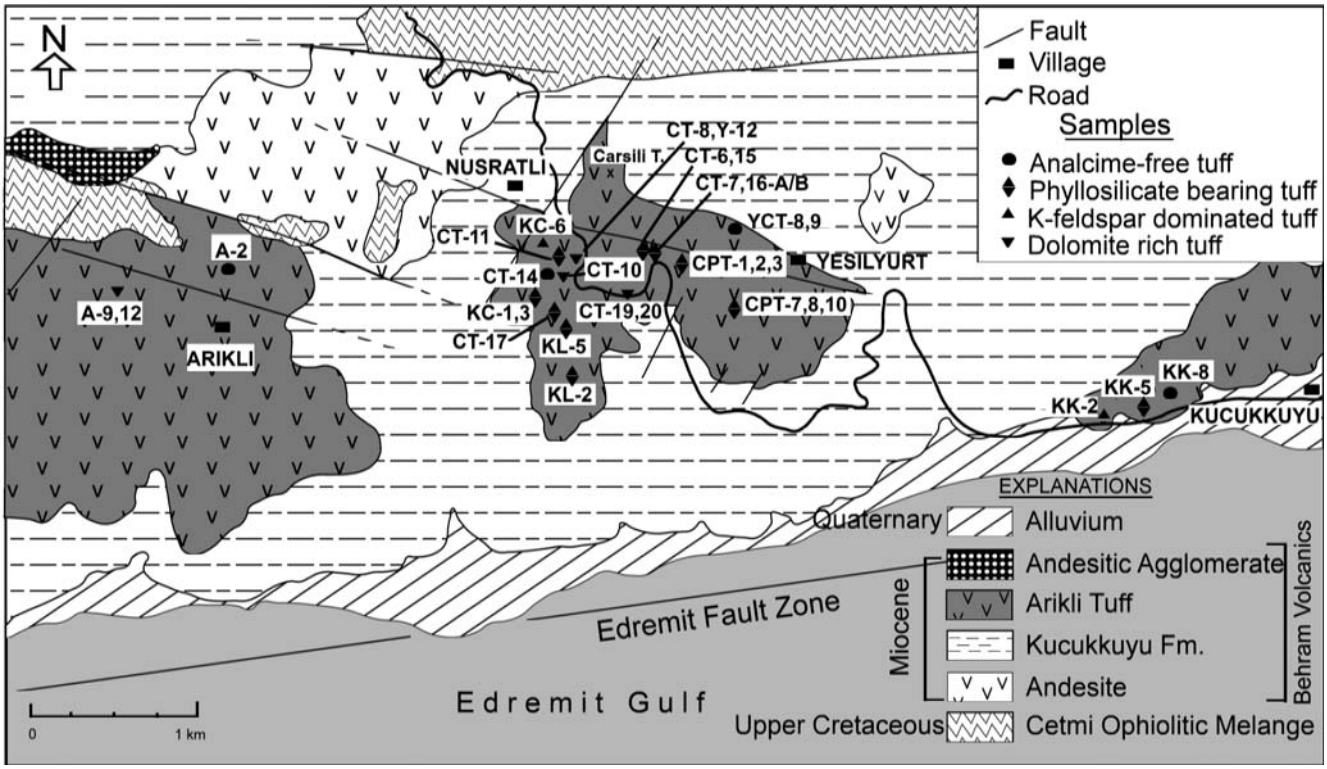

Fig. 2. Simplified geologic map of the Kucukkuyu area with sample locations (after Celik et al. 1999).

Analytical methods

From 50 tuff samples collected from different localities of the study area, 35 representative samples were studied in detail. The distribution of the samples is given in Fig. 2. The relative abundance of authigenic minerals was estimated by modal analyses. X-ray powder diffraction (XRD) analysis for the very fine-grained minerals was performed using a Rigaku D/Max-3 C diffractometer at General Directorate of Mineral Research and Exploration with a CuKα source operating at 40 kV/30 mA with a scan rate of 10 degree/min in the range of 0–70°. For detailed clay analysis, clay fractions in three samples were measured with a scan rate of 10 degree/min in the range of 0–25° by using Rigaku MiniFlex II diffractometer in the Department of Geological Engineering of METU with CuKα radiation, operating at 30 kV/15 mA. Clay minerals were identified according to the position of the (001) series of basal reflection on XRD patterns (air-dried at 25 °C, dissolved with ethylene glycol, heated at 300 °C for 1 h, and heated at 550 °C for 1 h). Thin sections of tuffs were examined to determine the texture and mineralogy. The grain size, morphology, actual three-dimensional crystal relationship, growth mechanism, and composition of analcime and other minerals were examined in gold-coated samples with a Jeol 6400 scanning electron microscope (SEM) equipped with an energy dispersive spectrometer (EDX) in Metallurgical and Materials Engineering Department and Quant 400 F in the Central Laboratory at METU. EDX was qualitatively used in order to determine semi-quantitatively the chemical composition of the glass-phase which controls the kind of zeolites formed. The relative abundance of minerals was estimated from optical, diffraction, and electron microscopy techniques. Inductively coupled plasma-optical emission spectrometry (ICP-OES) for major elements and inductively coupled plasma-mass spectrometry (ICP-MS) for trace elements and REE's analyses were used to determine the bulk chemistry of the Arikli Tuff in the ACME Analytical Laboratories at Canada. The results obtained for the major elements were recalculated including the loss of ignition (LOI). Mineral abbreviations are according to Kretz (1983).

Results

Petrography

The Arikli Tuff mainly consists of dust and ash-sized material and minor amounts of mineral clasts. Microscopical study reveals that the fragments range in size from

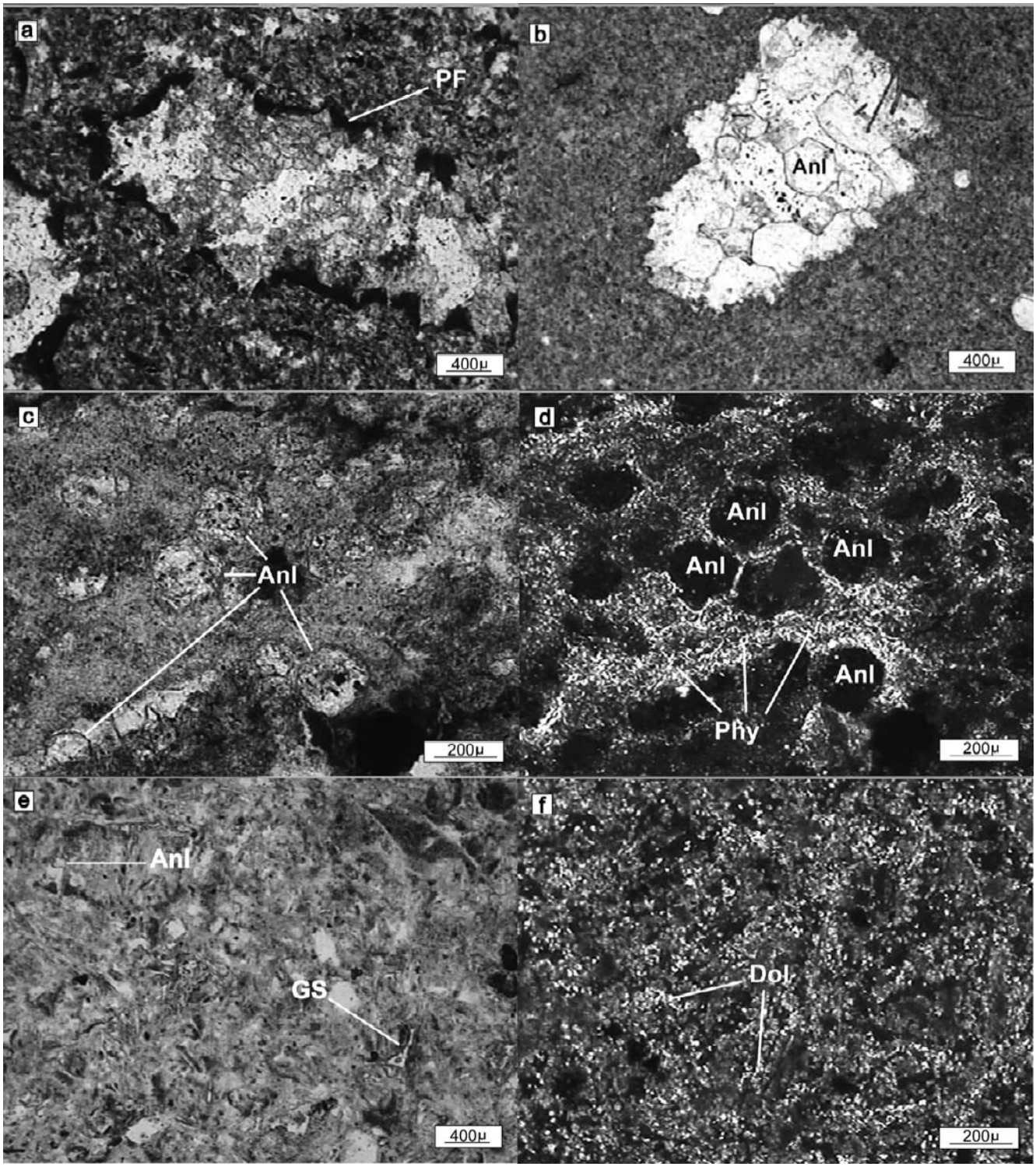

Fig. 3. Photomicrographs of (a) analcime crystals in a pumice fragment with a dark rim of very fine-grained Fe-oxide (CT-8, PPL); (b) trapezohedral analcime (colorless with low relief) in voids of dolostone (CT-10, PPL); (c) analcime clusters embedded in the matrix (KL-5, PPL); (d) isotropic analcime grains (XPL view of c); (e) analcime together with glass shard, (KK-2, PPL); (f) dolomite-rich vitric tuff (CT-8, XPL). PF = pumice fragment, Anl = analcime, Phy = phyllosilicate, Dol = dolomite, GS = glass shard.

Table 1. Relative phenocryst, lithic fragment and authigenic mineral abundances (+ relative abundance; – accessory; o not observed) in analcime-bearing Arikli Tuff.

	PHYLLOSILICATE BEARING VITRIC TUFF								
	primary minerals		vitric material		lithic fragments	authigenic minerals			
	quartz	biotite plagioclase sanidine	pumice fragment	glass shard	rock fragment	analcime	dolomite	phyllosilicate	K-feldspar
CT-6	–	–	+	○	–	++	○	+++	+
CT-7	+	+	–	○	–	++	–	+++	+
CT-11	+	+	–	○	–	++	○	+++	+
CT-15	+	–	–	○	–	++	○	+++	++
CT-16-A	–	–	–	○	–	++	–	+++	++
CT-16-B	–	–	+	○	–	++	○	++	++
CT-17	+	–	–	○	–	+	+	+++	++
YCT-8	+	–	–	○	–	○	○	+++++	+
CPT-1	+	+	–	○	–	++	+	++	++
CPT-2	+	+	+	○	○	++	○	++	++
CPT-3	+	–	–	○	○	+++	–	++	++
CPT-7	+	+	–	○	+	++	○	++	++
CPT-8	+	–	–	○	–	++	○	++	++
CPT-10	+	–	+	○	–	++	○	+++	++
KC-1	+	+	+	○	–	++	○	++	++
KC-3	+	+	+	○	–	++	○	++	++
KK-5	+	+	+	+	–	++	○	+++	+
KL-2	+	–	–	○	–	++	○	++	++
KL-5	+	+	+	○	+	++	○	++	++
	DOLOMITE RICH VITRIC TUFF								
	primary minerals		vitric material		lithic fragments	authigenic minerals			
	quartz	biotite plagioclase sanidine	pumice fragment	glass shard	rock fragment	analcime	dolomite	phyllosilicate	K-feldspar
A-9	+	–	+	○	–	++	+++	+	+
A-12	+	–	+	on	–	+	++++	–	+
CT-8	–	–	+	○	○	+++	+++	–	○
	Dolostone								
Y-12	–	–	○	○	○	++	++++	+	+
CT-10	–	–	○	○	○	++	++++	+	+
CT-19	–	–	○	○	○	++	++++	+	○
CT-20	–	–	○	○	○	++	++++	+	○
	K-FELDSPAR-DOMINATED VITRIC TUFF								
	primary minerals		vitric material		lithic fragments	authigenic minerals			
	quartz	biotite plagioclase sanidine	pumice fragment	glass shard	rock fragment	analcime	dolomite	phyllosilicate	K-feldspar
A-2	–	–	+	none	–	○	+	○	++++
KK-2	+	–	+	++	–	+	○	○	++++
KK-8	+	+	+	○	○	○	○	○	+++++
KC-6	+	–	+	○	–	+	○	+	++++
YCT-9	+	+	–	○	–	○	○	+	++++
	K–feldspar–dominated crystal tuff								
CT-14	+	++	–	○	–	○	+	+	++

0.01 mm to 0.06 mm, so the Arikli Tuff can be classified as fine (dust) tuff based on grain size (Fisher & Schmincke 1984). Tuff samples (except CT-14) were named as vitric tuff in terms of remnant glass shards and pumice fragments (Pettijohn 1975). Sample CT-14 is identified as crystal tuff, because of its phenocryst's content of 35 vol%. In addition, this sample contains fine-grained K-feldspar in the matrix determined by low birefringence and is grouped as K-feldspar-dominated crystal tuff. The primary composition of the Arikli Tuff can not be exactly determined by petrographic observations due to the diagenetic changes in mineralogy. Still, according to the abundances of the pheno- and micro-phenocrysts (Raymond 1995) the tuffs are rhyolitic to rhyodacitic in composition.

The primary minerals are quartz, minor biotite, plagioclase, and sanidine. The phenocryst content of vitric tuffs ranges from 2 to 18 vol%. Pumice fragments are usually elongate and some of them contain pores, which are mainly filled by analcime. These can be easily differentiated by a dark rim of very fine-grained Fe-oxide staining (Fig. 3a). Lath and Y-shaped glass shards are only found in two tuff samples (Table 1). Both samples KK-5 (phyllosilicate-bearing) and KK-2 (K-feldspar-dominated) are from the west of Kucukkuyu (Fig. 2). The general absence of volcanic glass is a striking feature and their absence has been attributed to the intense diagenetic alteration. Even though alteration prevents the exact determination of some fragments in the tuff samples, their ghost textures were used to recognize them as volcanic rock fragments. Except the phenocrysts, several compounds of the tuff (e.g. pumice fragments, glassy matrix and glass-shards) are altered by diagenesis. The cavities are sites of neo-mineralization. The diagenetic minerals are analcime, phyllosilicate, K-feldspar, and dolomite.

Petrographically analcime crystals are easily recognizable by their typical optical properties. They have low relief and are colorless (Fig. 3a, b, c), isotropic (Fig. 3d), and cubo-octahedral (Fig. 3b). Their sizes range between 100 µm to 1 mm in diameter. Two modes of occurrences of analcime are noticed; coarse-grained euhedral to subhedral crystals in pumice fragments (Fig. 3a) or in pores (Fig. 3b), and clusters or single crystals of fine-grained anhedral analcimes embedded in the matrix (Fig. 3c).

The presence of very fine-grained authigenic crystals scattered throughout the matrix can only be assured by XRD analysis, so that the modal amount of the authigenic mineral content (as volume %) on Table 1 is only a rough estimate. Microscopically, analcimes are mainly euhedral or subhedral in pumice fragments or voids and anhedral in the matrix. Thin sections of tuff demonstrate distinctly different stages of analcime precipitation in cavities ranging from quasi to complete filling. Analcimes are in general associated with secondary phyllosilicate, dolomite, and K-feldspar. Analcime in association with volcanic glass was observed in a few samples (e.g. samples KK-2 and KK-5; Fig. 3e). No textural evidence of replacement of any other zeolites, clay minerals, or feldspars by analcime was observed by optical or electronmicroscopic studies.

The tuffs are separated into three main groups on the basis of their authigenic mineral content visible and

Table 2. Mineralogy of Arikli Tuff samples determined by powder XRD (A = abundant, P = present, T = trace, N = not detected, Qtz = quartz, Anl = analcime, Kfs = K-feldspar, Dol = dolomite, Sm = smectite, Bt = biotite, Sa = sanidine).

	Qtz	Anl	Kfs	Dol	Sm	Bt	Sa
CT-6	P	P	P	N	P	T	N
CT-11	P	P	P	N	P	N	T
CT-8	P	P	N	P	T	N	N
A-12	P	P	P	A	T	N	N
A-9	P	P	P	P	P	N	T
KL-5	P	P	P	N	P	T	T
KK-5	P	P	P	N	P	N	T
CPT-3	P	P	P	N	P	T	T
CPT-2	P	P	P	N	P	T	T
KC-1	P	P	P	N	P	T	T
CT-17	P	P	P	N	P	T	T
CPT-1	P	P	P	N	P	N	T
CPT-7	P	P	P	N	P	N	T
CT-15	P	P	P	N	P	N	T
CT-7	P	P	P	N	P	N	T
CT-16-A	P	P	P	N	P	T	T
KK-2	P	P	A	N	N	N	T
CT-10	P	P	P	A	T	T	T
KC-6	P	P	A	N	P	N	T
KL-2	P	P	P	N	P	T	T
CT-19	P	P	T	A	T	N	N
KC-3	P	P	P	N	P	N	T
CPT-8	P	P	P	N	P	N	N
CPT-10	P	P	P	N	P	T	T
Y-12	P	P	P	A	T	T	N
CT-14	P	N	P	P	P	P	P
YCT-8	P	N	P	N	P	T	T
A-2	P	N	A	P	N	N	T
KK-8	P	N	A	N	N	N	N
YCT-9	P	N	A	N	P	T	T

Fig. 4. SEM images showing a) trapezohedral analcime with well-developed (211), (2$\bar{1}$1), (2$\bar{1}\bar{1}$), (21$\bar{1}$) and (100) faces and associated smectite showing honeycomb morphology (sample CPT-3); b) subhedral analcime grain (sample KL-5); c) analcime and quartz formation in voids; d) authigenic analcime overgrown on volcanic glass (sample A-12); e) euhedral quartz grains with well-developed (10$\bar{1}$1), (01$\bar{1}$1) and (10$\bar{1}$0) faces (sample CT-8); f) K-feldspar with well-developed (010) face (sample KK-2). ▶

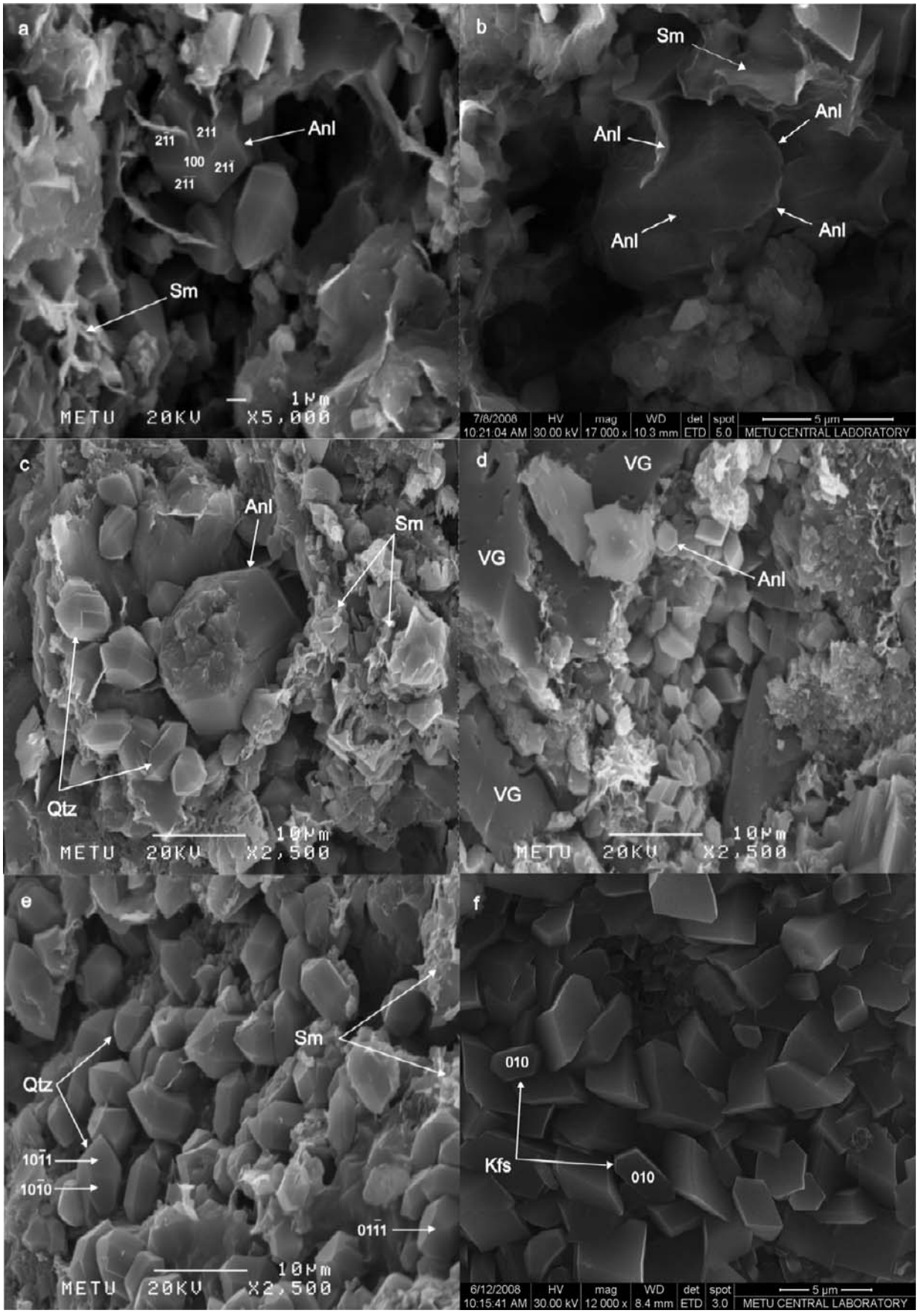
a
Anl
211
211
100
211
211
Sm
METU 20KV X5,000 1μm
b
Sm
Anl
Anl
Anl
Anl
Anl
7/8/2008 10:21:04 AM HV 30.00 kV mag 17 000 x WD 10.3 mm det ETD spot 5.0 5 μm METU CENTRAL LABORATORY
c
Anl
Sm
Qtz
METU 20KV X2,500 10μm
d
VG
VG
VG
Anl
METU 20KV X2,500 10μm
e
Sm
Qtz
10$\bar{1}$1
10$\bar{1}$0
01$\bar{1}$1
METU 20KV X2,500 10μm
f
010
Kfs
010
6/12/2008 10:15:41 AM HV 30.00 kV mag 12 000 x WD 8.4 mm det ETD spot 3.0 5 μm METU CENTRAL LABORATORY

dominant in the matrix; phyllosilicate-bearing vitric tuff (Fig. 3d), dolomite-rich vitric tuff (Fig. 3f), and K-feldspar-dominated vitric tuff (Ozen 2008, Ozen & Goncuoglu 2008). These three groups are similar in mineralogical character, but mineral or fragment abundances differ. The phyllosilicate-bearing tuffs are the most common ones and include lithic fragments and phenocrysts that are embedded in a matrix of μm-sized flakes of authigenic clay minerals. Phyllosilicates occurring as tiny crystals in the cryptocrystalline matrix were distinguished by their greenish yellow color and characteristic flaky appearance (Fig. 3d). The type of phyllosilicate was determined as smectite by the XRD and SEM analysis. The dolomite-rich vitric tuffs mainly occur at the contact of tuffs and sediments. They are characterized by the dominance of authigenic dolomite in the matrix. Disseminated dolomite grains occur as aggregates of anhedral habit (Fig. 3f). From this group, four samples (Y-12; CT-10; CT-19; CT-20) are free of tuffaceous material and were named as dolostones (Table 1). In sample CT-10, where no relict volcanic material is observed, cavities are filled with coarse-grained, euhedral to subhedral analcime crystals (Fig. 3b), indicating precipitation of analcime from pore fluids. The K-feldspar-dominated vitric tuff has a matrix with more than 65 vol% of very fine-grained K-feldspar crystals. K-feldspars are mainly anhedral in the matrix, but euhedral in pumice fragments. Although K-feldspars are differentiated by their low relief, low birefringence and mainly prismatic shape in thin-sections, their exact identification is mainly based on XRD and SEM studies.

Mineralogy

XRD analyses

Analcime, K-feldspar, dolomite, quartz, biotite, smectite, and sanidine are identified by XRD analyses (Table 2). This finding is in accordance with the microscopic observations. In the XRD-graphs, the characteristic peaks of analcime (2 θ of 25.97, 15.79, 30.50, 35.77, and 18.29 with *d*-spacings of 3.43, 5.62, 2.91, 2.50, and 4.85 Å, respectively) were clearly identified in samples. No other zeolite type was identified by the XRD analysis.

Dolomite can be identified by its typical 2.89, 2.19, 2.01, and 1.79 Å peaks, though its main peak overlaps the analcime (2.91 Å) peak. Quartz was identified by its 3.34, 4.26, 1.81, and 1.54 Å peaks. We used the K-feldspars peaks at 3.33, 3.79, 4.24, 3.23, 3.47, and 3.28 Å for identification (McClune 1991). The 3.33 and 4.24 Å peaks overlap with quartz. The 3.47 Å peak, however, can only be identified in analcime-free samples (e.g. CT-14) as it overlaps with analcime peak. In this respect, the exact type of K-feldspar is not determined. In CT-14 5.89 Å, 3.95 Å, 2.77 Å peaks are high-sanidine peaks. XRD patterns of air-dried, ethylene-glycolated and heated specimens (at 300 °C and 550 °C 1 hour) indicate the presence of smectite. Sample CT-14 includes a small

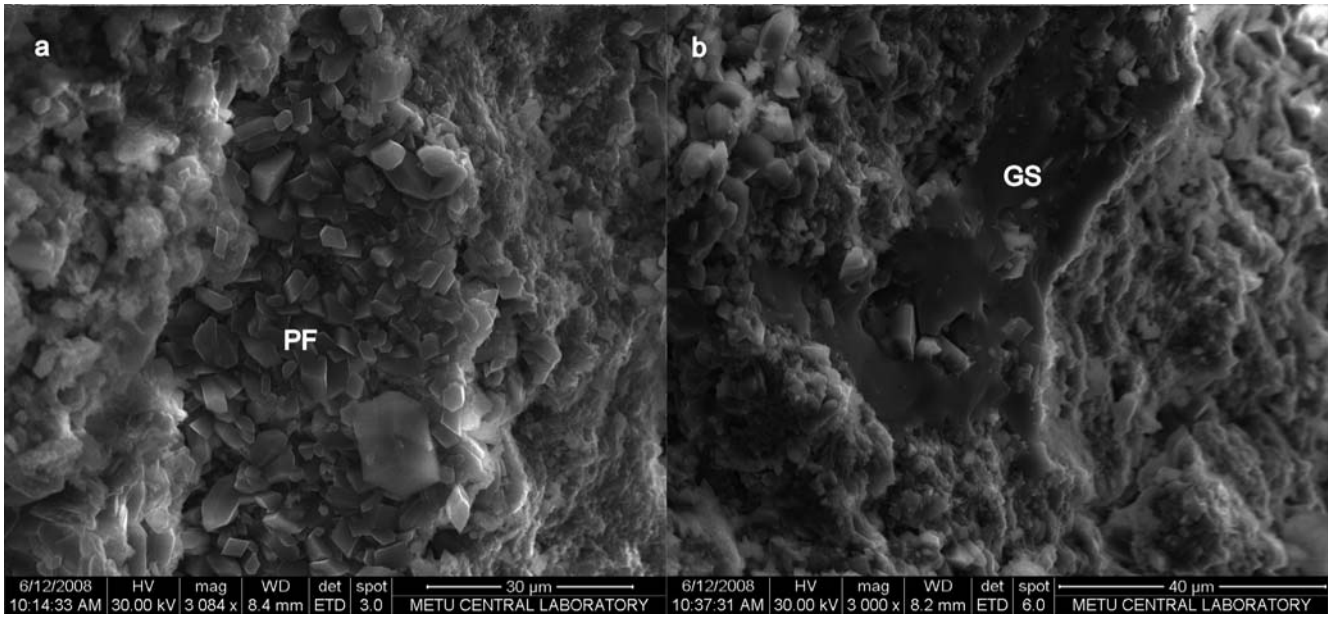

Fig. 5. SEM images showing a) an elongate pumice fragment (PF) with euhedral K-feldspar grains (sample KK-2); b) Y-shaped glass shard (GS; sample KK-2).

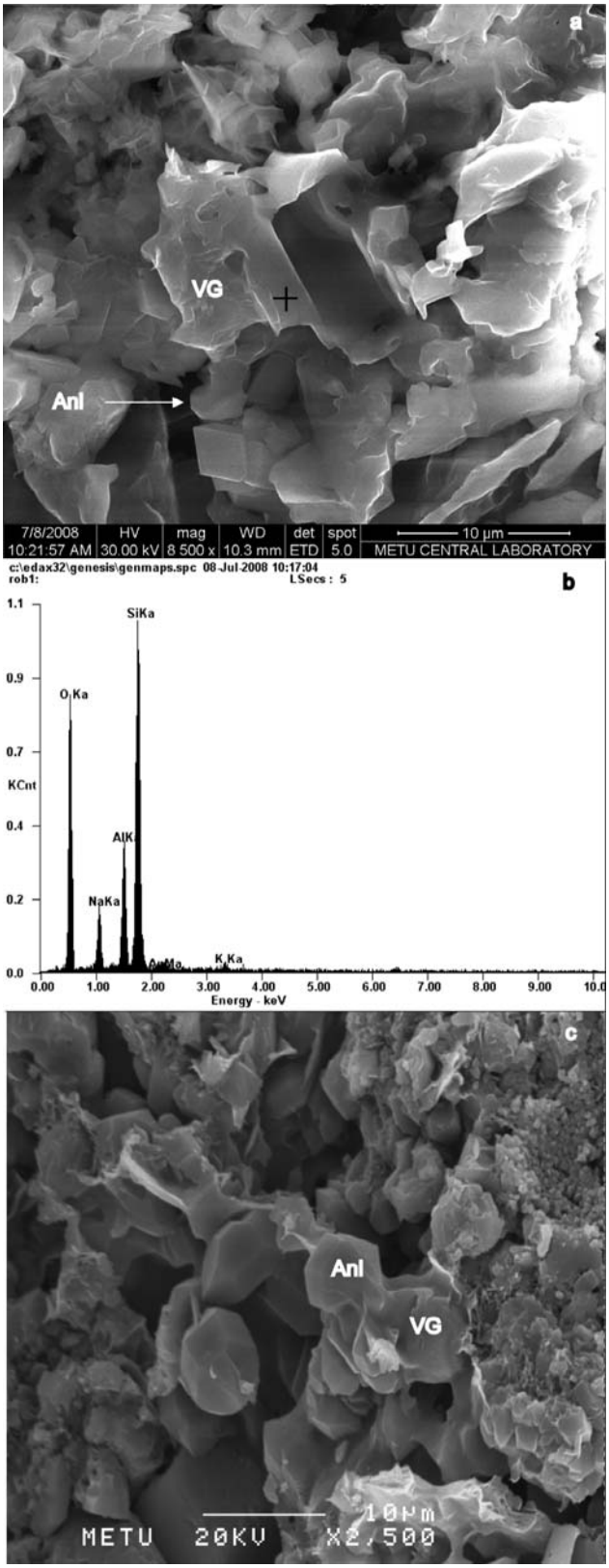

Fig. 6. SEM image (a) and EDX spectrum (b) of unaltered volcanic glass (VG) with subhedral analcime (Anl) on its edge (sample KL-5) and (c) SEM image of authigenic analcime overgrowth at the edge of volcanic glass (sample CT-8).

reflection of 10.12 Å in the random sample, which disappears in the air-dried or ethylene-glycolated sample, probably biotite.

SEM analyses

In Arikli Tuff, analcimes are present with well-developed trapezohedral faces (211), ($2\bar{1}$ 1), ($2\bar{1}\bar{1}$), ($21\bar{1}$), and (100) (Fig. 4a) and cubo-octahedral morphologies, recognized by their typical (111) faces. Subhedral analcime grains were also observed (Fig. 4b). The size of the analcime crystals ranges from 2 to 15 µm. They are observed in the relatively large pore spaces (Fig. 4c), and in contact with volcanic glass (Fig. 4d).

Identification of dolomite is based on its rhombic morphology. The size of dolomite crystals ranges from 2 to 5 µm. Some of them can display twining. In SEM images, quartz can be easily differentiated by its right or left trigonal trapezohedral morphology with well-developed ($10\bar{1}$ 1), ($01\bar{1}$1), and ($10\bar{1}$0) faces (Fig. 4e). Analcime crystals are generally associated with smectite (Fig. 4a, b). While K-feldspars appear in monoclinic morphology with well-developed (010) faces (Fig. 4f), smectites exhibit a honeycomb arrangement, a typical crystal habit (Fig. 4a, b, c).

Pumice fragments can be easily differentiated from matrix by their texture (Fig. 5a). They are 20–60 µm wide and 70–130 µm long. In SEM images, porous and amorphous glass shards were recognized in the tuff (Fig. 4d). Typical Y-shaped volcanic glass shards are 20 µm wide and 70 µm long (Fig. 5b). Analcime occurs as subhedral crystals at the edges of the glass shards. For volcanic glasses, qualitative chemical analysis by EDX was performed to control its composition (Karakas & Kadir 2006). This application is of importance, beause the type of the newly formed zeolite is controlled by the chemistry of the glass. Thus, EDX was applied on unaltered surface of glass which subhedral analcime found on the edge of the glass (Fig. 6a). The EDX spectrum contains the typical components in analcime Na, Al, and Si and additionally K (Fig. 6b). Figure 6 c is the best view of the authigenic analcime overgrows the edge of volcanic glass which shows the alteration of volcanic glass.

Geochemistry

Whole-rock major oxide and trace element analysis were used to determine chemical changes within the studied tuff deposits to compare them with the parent material from which they were derived. Twenty representative samples were selected to study the geochemical features of the Arikli Tuff (Table 3). The abundances of Na, K, Mg, and Ca oxides vary widely from 0.13 to 5.88 wt% for

Table 3. Major (wt%) and trace element (ppm) values of Arikli Tuff (ΣFe_2O_3 as total iron, LOI = Loss on ignition at 1000 °C).

wt %/sample	CT-6	CT-7	CT-11	CT-15	CT-16-A	CT-17	CPT-1	CPT-3	CPT-7	CPT-10	KC-1	KK-5	KL-5	A-9	A-12	CT-8	Y-12	A-2	CT-14	YCT-9
	phyllosilicate bearing vitric tuff													dolomite rich vitric tuff				K-felds-dominated v.t.		
SiO_2	64.3	65.77	66.62	65.2	65.91	66.13	64.63	66.36	67.96	68.94	66.17	63.39	65.91	54.5	51.22	52.85	57.38	66.19	64.12	67.89
Al_2O_3	15.36	14.33	14.29	14.64	14.43	13.96	13.85	14.54	13.65	13.18	14.65	15.06	15.09	12.9	10.63	12.11	13.28	14.04	15	14.31
Fe_2O_3	1.99	2.36	2.47	2.17	2.06	2.24	2.13	2.24	2.27	2.26	2.33	2.49	1.74	1.93	1.85	1.91	2.98	1.78	2.87	2.4
MgO	0.91	1.18	0.58	1.25	1	1.17	1.4	0.8	0.86	0.7	0.98	1.38	0.63	3.83	5.03	4.7	3.06	1.15	1.1	0.56
CaO	0.6	0.56	0.28	0.45	0.69	0.69	0.77	0.5	0.51	0.33	0.27	0.82	0.44	5.37	8.14	5.92	3.62	1.72	0.63	0.16
Na_2O	4.11	3.52	4.33	3.91	3.77	2.95	3.26	3.62	3.04	3.33	3.75	2.58	3.28	3.1	3.57	5.88	1.58	0.13	0.56	0.24
K_2O	5.33	6.11	5.1	5.18	5.19	6.16	6.6	6.74	6.45	5.51	6.68	4.46	6.05	5.58	3.32	0.8	7.47	9.47	12.19	11.84
MnO	0.04	0.02	0.04	0.03	0.05	0.03	0.03	0.05	0.04	0.02	0.03	0.03	0.03	0.11	0.18	0.1	0.08	0.05	0.01	0.02
TiO_2	0.35	0.33	0.33	0.32	0.33	0.32	0.33	0.34	0.33	0.31	0.34	0.36	0.31	0.29	0.26	0.27	0.38	0.32	0.5	0.33
P_2O_2	0.06	0.069	0.057	0.054	0.049	0.057	0.07	0.056	0.066	0.052	0.06	0.07	0.072	0.06	0.045	0.143	0.132	0.061	0.11	0.051
LOI	6.7	5.4	5.7	6.7	6.5	6.2	6.9	4.7	4.7	5.2	4.6	9.1	6.4	12.1	15.5	15.2	9.6	5	2.7	2
Total	99.76	99.64	99.79	99.91	99.95	99.91	99.93	99.93	99.86	99.84	99.82	99.76	99.91	99.8	99.75	99.89	99.53	99.86	99.81	99.77
ppm																				
Y	22.8	20.8	25.7	18.8	19.7	19.8	21.6	22.4	27.7	29.8	25.5	27.1	22.2	23.2	22.6	21.6	23.5	24.4	21.8	25.2
Nb	22.1	21.2	21.8	20.4	20.1	20.5	21.3	21	21.5	21.1	21.1	23.3	17.3	16.8	14.5	17.3	16.3	20	17.9	21.6
Zr	388.6	390.6	401.1	316.7	377.9	352	398.7	410.5	406.4	394	380.4	355.7	434.7	287	233.9	292	276.2	323.5	350.1	406

Na_2O; 0.80 to 12.19 wt% for K_2O; 0.56 to 5.03 wt% MgO, and 0.16 to 8.14 wt% for CaO indicating their mobility during alteration (Table 3).

Because analcime contains water, analcime-bearing tuffs have higher LOI values than analcime-free samples. A good correlation between CaO and LOI is seen in all dolomite rich samples (A-9; A-12; Y-12; CT-8), which have the highest LOI values. Therefore the analcime-free dolomitic tuffs (e.g. sample A-2) have a higher LOI value (1.72 wt. %) than other analcime-free tuffs.

To determine the nature of the host rock affecting the type of zeolites formed (*e.g.* Kitsopoulos et al. 2001) the chemical data were plotted on the Nb/Y vs. Zr/TiO_2 discrimination diagram of Winchester & Floyd (1977). From the trace elements, Zr and Ti are considered as immobile trace elements. Y, on the other hand, can be mobile under high diagenetic temperatures (Finlow-Bates & Stumpfl 1981, Kitsopoulos et al. 2001). Therefore, the position of some samples on the Winchester & Floyd (1977) diagram could have been affected by the mobilization of Y during the alteration of glass and the composition of the parent rocks is shifted towards the field of trachyandesite (Fig. 7). Besides, the Arikli Tuff was petrographically determined as rhyolitic to rhyodacitic in composition with respect to phenocryst content. Thus, its true nature could actually be closer to rhyolite-dacite, thus controlling the chemical composition and type of zeolitization.

Arikli Tuff samples plotted in the elemental abundance diagram clearly reveals the presence of three distinct groups as readily discriminated by petrographical observations (Fig. 8). Samples of white circles with the highest K and lowest Na values were differentiated as K-feldspar-dominated vitric tuff and all samples of this group are analcime-free. Even though there is no exact

Fig. 7. Arikli Tuff samples on the Zr/TiO_2 vs Nb/Y discrimination diagram (Winchester & Floyd 1977)

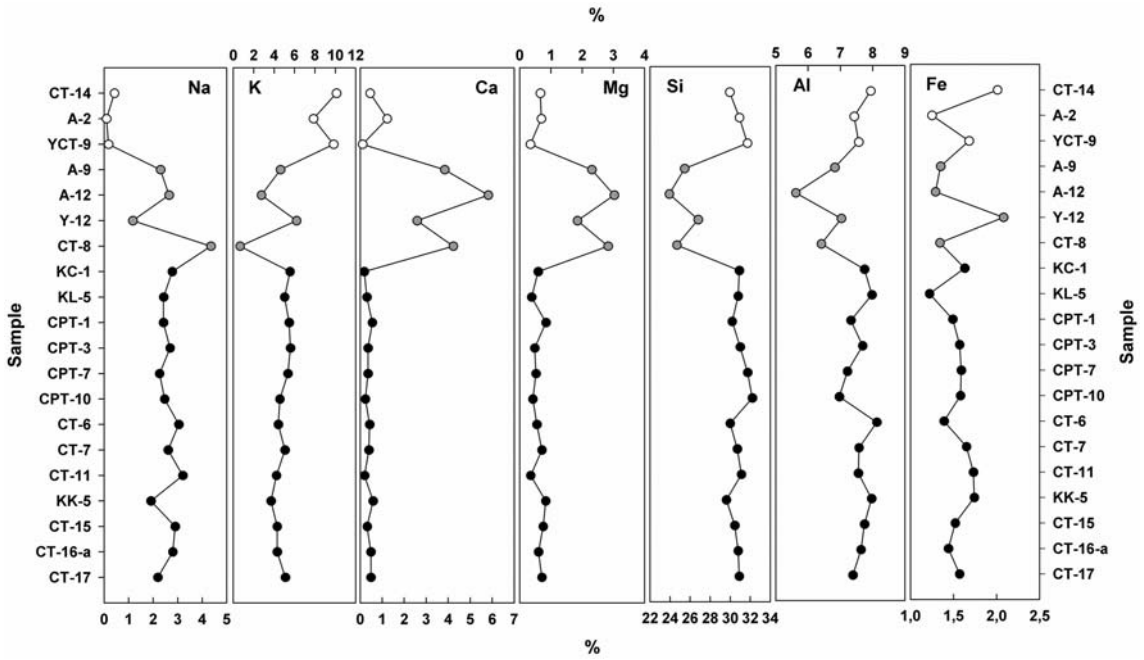

Fig. 8. Major element abundances of samples from Arikli Tuff (white circles are K-feldspar-dominated vitric tuff, gray circles are dolomite-rich vitric tuff and black circles are phyllosilicate-bearing vitric tuff) in wt% oxides

reverse relationship between Na and K, it can be noticed that studied samples with higher K usually contain lower Na or vice versa. The mobilization of alkalies under diagenetic conditions is common (Kitsopoulos et al. 2001). Thus, it is not surprising that the alteration process was associated with the removal of Na and enrichment of K in analcime-free samples. The low Na content in these samples can be also explained by the absence of analcime. Gray circles differentiated with higher Ca, Mg but low Si, Al contents coincide with dolomite-rich vitric tuff and dolostone. In addition, sample CT-8 has the highest Na and lowest K content. Remaining phyllosilicate-bearing vitric tuff samples (black circles) display a rather smooth line (Fig. 8). There is little or no change in Fe content. The change from the rhyolitic precursor to the analcime-bearing tuff seems to involve a diffusion-controlled hydration, as clearly observed on Figure 8 showing the relative gain and losses of elements (Kitsopoulos et al. 2001).

Occurrence of analcime

The major controls on the formation of zeolites in volcaniclastic sediments are a high proportion of glassy particles, favorable hydrological conditions, and high internal surface area (Hall 1998) of the source material. Several additional factors can affect the type of zeolite formed when pore solutions react with glassy material in the parent rock. These factors are salinity, alkalinity (pH), relative proportions of the alkali and alkaline earth cations, initial composition of host rock, pressure, temperature, and time (Ratterman & Surdam 1981, Sheppard & Gude 1968, Hay 1966, Iijima & Hay 1968). Among them, the chemical composition of starting material is one of the most important parameters to designate the kind of zeolite formed. For instance, rhyolitic glasses, as it is the case in Arikli Tuff, mostly favor the crystallization of analcime and mordenite if other conditions are also appropriate (Holler & Wirsching 1978).

Generally, analcime can be formed by replacement of earlier alkali zeolites derived from glassy material (Hay 1966, Iijima & Hay 1968, Sheppard & Gude 1968, Surdam & Sheppard 1978). However, there is no evidence about the presence of precursor zeolites in Arikli Tuff. One possibility, however, is that all these zeolites were completely altered to analcime, leaving no evidence of their former existence. In addition to alkali zeolites, clay minerals and feldspars are also proposed as precursors of analcime, but again no textural evidence of analcime formation through these minerals was found in the Arikli Tuff.

In the absence of pyroclastic material, direct precipitation of analcime from lake water, where zeolites are laterally widespread is suggested by several authors (e.g. Hay 1966, Wu 1970, Renaut 1993, English 2001). In most of these cases, analcime is the dominating phase and forms thin layers (e.g. Karakas & Kadir 2006). However, in

the studied samples, analcime is identified only in pore spaces of dolostones. Furthermore, laterally expanding analcime beds even as very thin layers are not observed in both dolostones and tuffs. Therefore, direct precipitation by evaporation is excluded. By this, it may be considered that the studied analcimes were formed by precipitation from interstitial pore fluids, but not connected to evaporation of lake water. The occurrence of coarse-grained subhedral analcime crystals in pores of pumice fragments (Fig. 3a) and euhedral analcime crystals in pores of dolostone (Fig. 3b) clearly shows that analcime was formed by precipitation from pore water, where the dissolved components were concentrated. The mechanism can be explained by spontaneous nucleations from supersaturated pore solution and following growth of analcime crystal. As dolostones are originally devoid of glassy fragments, the source of Na is probably circulating saturated pore water. According to Wu (1970) the chemical precipitation of analcime is a function of pH, salinity, and Na availability. Because Na is one of the most abundant ions in saline, alkaline-lakes (Eugster & Hardie 1978), the circulating water, which is rich in Na ions, is easily precipitated in voids of dolostones and tuffs and form euhedral to subhedral analcimes (Chipera & Apps 2001, Birsoy 2002) .

Another zeolite-forming process in nature is zeolitization of volcanic glass (High & Picard 1965, Iijima & Utada 1966, Larsen et al. 1991). The state-of-art interpretations on this process are mainly based on experimental work on analcime syntheses from natural or synthetic glasses in simplified systems compared with the complex conditions of natural processes (Aiello et al. 1971, Larsen et al. 1991, Fang et al. 2004). Moreover, the glass dissolution and analcime crystallization may be complicated, as dissolution and nucleation reactions involve a large number of steps and reactive species (Fang et al. 2004). This is further complicated by the chemically inhomogeneous character of tuffs. However, these experimental data can provide an overall insight to the processes involved.

The formation of analcime in tuffaceous material commonly results from the diagenetic alteration of volcanic glass (e.g. High & Picard 1965). The association of analcime (Fig. 3e) with relict glass shards, pumice fragments etc. (samples KK-2; KK-5) in the Arikli Tuff is in favor of such a formation. Moreover, disseminated fine-grained anhedral analcime aggregates are embedded within the matrix of the altered tuff. These aggregates include sometimes isotropic cryptocrystalline analcime. This type of analcime dominates over coarse-grained pore-filling ones in all studied samples.

Besides, the SEM images of the Arikli Tuff clearly indicate that authigenic analcime crystal formed at the edge of volcanic glass (Fig. 6a). The textural relationship between volcanic glass and subhedral analcime is also obvious (Fig. 6c). Here subhedral analcime is grown on the surface of glass. The occurrence of analcime in contact with glass supports our suggestion that nucleation and crystal growth might be the result of dissolution and Na, Al, Si, and K fluctuations from the glass and in situ crystallization of analcime.

Nucleation of analcime at or near the glass might be affected by several processes. Fang et al. (2004) proposed a theoretical model to show that the growth of nuclei was basically controlled by the solution concentration. When the solution reaches its supersaturation, nucleation of analcime might have occurred spontaneously. The other controlling factors are pH, environmental alkalinity, pressure, and temperature. (Hay 1966, Iijima & Hay 1968, Sheppard & Gude 1968, Ratterman & Surdam 1981).

The formation from glass was not only recognized in SEM images but is also supported by the EDX spectrum of the samples which shows that volcanic glass in Arikli Tuff is chemically suitable for the formation of analcime (Fig. 6b). In this case as far as the chemical composition is concerned, a remarkable similarity between analcime and volcanic glass is evident. Occurrence of analcime by dissolution-precipitation of glass is the most likely hypothesis, because of the high reactivity of volcanic glass and most importantly the chemical similarity between analcime and the volcanic glass. Therefore we argue that nucleation occurs at sites of dissolved glass, and that crystal growth involves a polymerization of continued dissolved nutrients on these growing surfaces. Essentially, analcime can nucleate anywhere in the system. However, dissolving glass supplies a high flux of Na, Al, Si, and K ions, and analcime will mainly nucleate on or close to the glass surfaces (Fig. 4d, 6 a, 6 c).

In summary, two modes of occurrence of analcime were observed; coarse-grained euhedral to subhedral analcime crystals in pores and pumice fragments and fine-grained anhedral crystals embedded in the matrix. Occurrence of analcime coating pores and the absence of glassy material indicate that analcime precipitated from pore water. Fine-grained anhedral analcime crystals disseminated in matrix were formed from dissolution of highly reactive volcanic glass and subsequent in-situ precipitation of analcime. As a result of dissolution of volcanic glass, the enrichment of Na, Al, Si, and K ions into the fluid phase accelerated the formation of analcime.

Acknowledgments

This study was funded by METU-OYP. We appreciate Dr. M. Albayrak's (MTA) contribution for sharing his knowl-

edge on the field localities, comments and suggestions on the XRD data and SEM images, realized in METU Central Laboratory. Drs. H. Yalcin (Sivas), S. Kadir (Eskişehir) and G. D. Gatta (Milano) are acknowledged for their valuable comments on the manuscript. An earlier version of the manuscript has benefited by the critical review of Dr J. W. Stucki (Illinois). Finally, we gratefully acknowledge the comments and corrections of Drs. F. Esenli (Istanbul), R. Birsoy (Izmir) and the Assoc. Editor G. Franz (Berlin) on the manuscript.

References

Abdioğlu, E. (2011): Mineralogy and chemistry of zeolites and associated minerals in Tertiary alkaline volcanics from the Eastern Pontides, NE Turkey. – N. Jb. Min. Abh. **184**: (in press).

Aiello, R., Colella, C. & Sersale, R. (1971): Zeolite formation from synthetic and natural glasses. – Adv. in Chem. Series **101**: 51–58.

Ataman, G. & Gundogdu, N. (1982): Analcimic zones in the Tertiary of Anatolia and their geological positions. – Sediment. Geol. **31**: 89–99.

Bingol, E., Akyurek, B. & Korkmazer, B. (1973): Geology of the Biga peninsula and some features of the Karakaya formation. Proceedings, Congress 50. Anniversary of Turkish Republic, 70–76.

Birsoy, R. (2002): Activity diagrams of zeolites: implications for the occurrences of zeolites in Turkey and of erionite worldwide. – Clays and clay minerals **50**: 36–144.

Borsi, S., Ferrara, C., Innocenti, F. & Mazzudi, R. (1972): Geochronology and petrology of recent volcanics of Eastern Aegean Sea. – Bull. of Volcanology **36**: 473–496.

Celik, E., Ayok, F. & Demir, N. (1999): Phosphate mineralization in Ayvacik-Kucukkuyu (Canakkale Province). – General Directorate of Mineral Research and Exploration Open File Report No: 10228.

Chipera, S. J. & Apps, J. A. (2001): Chemical stability of Natural Zeolites. – Reviews in Mineral. and Geochem. **45** (1): 17–161.

Ciftci, N. B., Temel, R. O. & Terzioglu, M. N. (2004): Neogene stratigraphy and hydrocarbon systematics around Edremit Bay. – Assoc. of Turkish Petroleum Geologists Bull. **16** (1): 81–104.

English, P. M. (2001): Formation of analcime and moganite at Lake Lewis, central Australia: significance of grounwater evolution in diagenesis. – Sediment. Geol. **143**: 219–244.

Ercan, T., Satir, M., Steinitz, G., Dora, A., Sarifakioglu, E., Adis, C., Walter, H. J. & Yildirim, T. (1995): Features of the Tertiary volcanism in Biga peninsula, Gokceada, Bozcaada ve Tavsan islands (NW Anatolia). – Miner. Research and Exploration Bull. **117**: 55–86.

Esenli, F. & Ozpeker, I. (1993): Gordes cevresindeki neojen havzanın zeolitik diyajenezi ve hoylandit-klinoptilolitlerin mineralojisi. – Turkiye Jeoloji Kurultayı Bulteni, p. 8–18.

Esenli, F., Uz, B., Suner, F., Esenli, V., Ece, Ö. I. & Kumbasar, I. (2005): Zeolitization of tuffaceous rocks in the Keşan region, Thrace, Turkey. – Geologia Croatica **58/2**: 51–161.

Eugster, H. P. & Hardie, L. A. (1978): Saline lakes. – In: Lerman, A. (Ed.): Lakes: Chemistry, Geology and Physics. – Springer Verlag, New York.

Fang, J. N., Lin, I. C., Lo, H. J., Song, S. R. & Chen, Y. L. (2004): The kinetics of analcime synthesis in alkaline solution. – J. of the Chinese Chem. Soc. **51**: 267–1272.

Finlow-Bates, T. & Stumpfl, E. F. (1981): The behavior of so-called immobile elements in hydrothermally altered rocks associated with volcanogenic submarine-exhalative ore deposits. – Miner. Depos. **16**: 319–328.

Fisher, R. V. & Schmincke, R. V. (1984): Pyroclastic Rocks. – Springer-Verlag, Berlin, 472 pp.

Goncuoglu, M. C., Dirik, K. & Kozlu, H. (1997): General characteristics of pre-Alpine and Alpine Terranes in Turkey: Explanatory notes to the terrane map of Turkey. – Ann. Géologiques des Pays Hélléniques **37**: 515–536.

Gundogdu, M. N., Yalcin, H., Temel, A. & Clauer, N. (1996): Geological, mineralogical and geochemical characteristics of zeolite deposits associated with borates in the Bigadic, Emet and Kırka Neogene lacustrine basins, western Turkey. – Miner. Deposit. **31**: 492–513.

Hall, A. (1998): Zeolitization of volcaniclastic sediments: The role of temperature and pH. – J. of Sediment. Research **68** (5): 739–745.

Hay, R. L. (1966): Zeolites and zeolitic reactions in sedimentary rocks. – Geol. Soc. of America Spec. Papers **85**: 30.

Hay, R. L. & Sheppard, R. A (2001): Occurrence of zeolites in sedimentary rocks: An overview. – In: Bish, D. L. & Ming, D. W. (eds.): Natural Zeolites: Occurrence, Properties, Applications. pp. 217–234; Mineral. Soc. of America, Washington.

High, L. R. & Picard, M. D. (1965): Sedimentary petrology and origin of analcime-rich Popo Agie member, Chugwater (Triassic) formation, west-central Wyoming. – J. of Sedimentary Petrol. **35** (1): 49–70.

Holler, H. & Wirsching, U. (1978): Experiments on the formation ofzeolites by hydrothermal alteration of volcanic glasses. – In: Sand L. B. & Mumpton, F. A. (eds.): Natural Zeolltes, Occurrence, Properties, Use. pp. 329–336; Pergamon Press, Elmsford, New York.

Iijima, A. & Hay, R. L. (1968): Analcime composition in tuffs of the Green river formation of Wyoming. – The American Mineralogist **53**: 84–200.

Iijima, A. & Utada, M. (1966): Zeolites in sedimentary rocks, with reference to the depositional environments and zonal distribution. – Sedimentology **7**: 327–357.

Inci, U. (1984): Stratigraphy and organic material contents of Demirci ve Burhaniye bituminous shales. – Bull. of the Geol. Soc. of Turkey **5**: 27–40.

Karakas, Z. & Kadir, S. (2006): Occurrence and origin of analcime in a Neogene volcano-sedimentary lacustrine environment, Beypazarı-Cayırhan basin, Ankara, Turkey. – N. Jb. Mineral. Abh. **182**: 253–264.

Kitsopoulos, K. P., Scott, P. W., Jeffrey, C. A., & Marsh, N. G. (2001): The mineralogy and geochemistry of zeolite-bearing volcanics from Akrotiri (Santorini Island) and Polyegos (Milos group of islands), Greece: Implications for geochemical classification diagrams. – Bull. of the Geol. Soc. of Greece **34** (3): 859–865.

Kretz, R. (1983): Symbols for rock-forming minerals. – American Mineralogist **68** (1/2): 277–279.

Larsen, G., Plum, K. H. & Forster, H. (1991): Zeolites and other hydrothermal alteration pruducts of synthetic glasses. – Europ. J. of Mineral. **3**: 933–941.

McClune, W. F. (1991): Powder diffraction file: inorganic. – Joint Committee on Powder Diffraction Standards. U.S.A.

Okay, A. I., Siyako, M. & Burkan, K. A. (1990): Geology and tectonic evolution of the Biga peninsula. – Assoc. of Turkish Petroleum Geologists Bull. **2**: 83–121.

Ozen, S. (2008): Mineralogical, petrographical and geochemical properties of zeolite bearing tuffs in NW Anatolia (Turkey). – MSc thesis, Middle East Technical University, Turkey, 188 pp.

Ozen, S. & Goncuoglu, M. C. (2009): Mineralogical, petrographical and geochemical properties of analcimes in Miocene tuffs in Kucukkuyu (Biga Peninsula). – 62nd Geological Kurultai of Turkey **19**: 605.

Pettijohn, F. J. (1975): Sedimentary Rocks. – 2nd Ed., New York, Harper and Row, 718 p.

Ratterman, N. G. & Surdam, R. C. (1981): Zeolite mineral reactions in a tuff in the Laney member of the Green River formation. – Wyoming. Clays and Clay Minerals **29**: 365–377.

Raymond, L. A. (1995): Petrology: The study of igneous, sedimentary and metamorphic rocks. – WCB/McGraw-Hill, 742 p.

Remy, R. R. & Ferrel, R. E. (1989): Distribution and origin of analcime in marginal lacustrine mudstones of the Green River Formation, south-central Uinta Basin, Utah. – Clays and Clay Minerals **37**(5): 419–432.

Renaut, R. W. (1993): Zeolitic diagenesis of late Quaternary fluviolacustrine sediments and associated calcrete formetion in the Lake Bogoria Basin, Kenya Rift Valley. – Sedimentology **40**: 271–301.

Sheppard, R. A. & Gude, A. J. (1968): Distribution and genesis of authigenic silicate minerals in tuffs of Pleistocene Lake Tecopa, Inyo Country, California. – U. S Geol. Survey Professional Paper **597**, p. 38.

Siyako, M., Burkan, K. A. & Okay, A. I. (1989): Tertiary geology and hydrocarbon possibilities of Biga and Gelibolu peninsula. – Assoc. of Turkish Petroleum Geol. Bull. **3**: 83–199.

Surdam, R. C. & Sheppard, R. A. (1978): Zeolites in saline, alkaline-lake deposits.– In: Sand, L. B. & Mumpton, F. A. (eds.): Natural Zeolites: Occurrence, properties, use; pp. 145–174; Pergamon Press, Elmsford, New York.

Winchester, J. A. & Floyd, P. A. (1977): Geochemical discrimination of different magma series and their differentiation products using immobile elements. – Chem. Geol. **20**: 325–343.

Wu, D. C. (1970): Origin of mineral analcite in the upper flowerpot shale, northwestern Oklahoma. – Transactions of the Kansas Acad. of Science **73** (2): 247–251.

Yilmaz, Y., Genc, S. C., Karacik, Z. & Altunkaynak, S. (2001): Two contrasting magmatic associations of NW Anatolia and their tectonic significance. – J. of Geodynamics **31**: 243–271.

Submitted: January 26, 2011; accepted: July 15, 2011.
Responsible editor: G. Franz

Author's addresses:

Sevgi Ozen, Middle East Technical University, Department of Geological Engineering, 06531, Ankara, Turkey. E-mail: ozsevgi@metu.edu.tr

M. Cemal Goncuoglu, Middle East Technical University, Department of Geological Engineering, 06531, Ankara, Turkey. E-mail: mcgoncu@metu.edu.tr